Design and implementation of a computer vision-guided greenhouse crop diagnostics system

Article *in* Machine Vision and Applications · May 2015
DOI: 10.1007/s00138-015-0670-5

2 authors, including:

Murat Kacira
The University of Arizona
77 PUBLICATIONS **997** CITATIONS

SEE PROFILE

Machine Vision and Applications (2015) 26:495–506
DOI 10.1007/s00138-015-0670-5

ORIGINAL PAPER

Design and implementation of a computer vision-guided greenhouse crop diagnostics system

David Story · Murat Kacira

Received: 2 May 2014 / Revised: 9 October 2014 / Accepted: 22 February 2015 / Published online: 19 March 2015

Abstract An autonomous computer vision-guided plant sensing and monitoring system was designed and constructed to continuously monitor temporal, morphological, and spectral features of lettuce crop growing in a nutrient film technique (NFT) hydroponics system. The system consisted of five main components including (1) a stepper motor-driven camera positioning system, (2) an image acquisition system, (3) a data logger monitoring root and aerial zone of the growing environment, (4) a dynamic SQL database module for data storage, and (5) a host computer running the collection, processing, storage, and analysis functions. Panoramic canopy images were dynamically created from the images collected by color, near-infrared (NIR) and thermal cameras. From these three images, the crop features were registered such that a single extracted crop (or a crop canopy) contained information from each layer. The extracted features were color (red–green–blue, hue-saturation-luminance, and color brightness), texture (entropy, energy, contrast, and homogeneity), Normalized Difference Vegetative Index (NDVI) (as well as other similar indices from the color and NIR channels), thermal (plant and canopy temperature), plant morphology (top projected plant and canopy area), and temporal changes of all these variables. The computer vision-guided system was able to extract these plant features and stored them into a database autonomously. This paper introduces the engineering design and system components in detail. The system's capability is illustrated with a one-day sample of the lettuce plants growing in the NFT system, presenting the temporal changes of three key crop features extracted, and identification of a stress level and locality detection as example applications.

D. Story · M. Kacira (✉)
Department of Agricultural and Biosystems Engineering,
University of Arizona, Tucson, AZ 85721-0038, USA
e-mail: mkacira@email.arizona.edu

Keywords Computer vision · Crop monitoring · Data acquisition · Greenhouse · Image processing

1 Introduction

Understanding how plants interact with their surrounding environment is essential for improved climate control strategies and management in greenhouse plant production systems. Traditionally, environmental parameters in greenhouses such as air temperature, humidity, and carbon dioxide concentrations are monitored and controlled by sampling at a single location as being representative of average conditions in the greenhouse. Thus, the macroclimate is controlled. However, the microclimate at the plant and leaf boundary layer controls the exchange processes. Furthermore, the microclimate is influenced not only by the macroclimate but also by the physical state of the plants. Therefore, the systems having the most direct effect on greenhouse microclimate can be superior in terms of resource use efficiency.

By monitoring plant's responses under a given environmental condition, the data derived from crop monitoring can be used to compare crops over time and space, enhancing the information for greenhouse climate control. However, a crop monitoring system should be capable of recording data continuously, automatically, and non-invasively if it will be used in a commercial greenhouse setting, especially for real-time monitoring, decision support, and control applications. Additionally, the system must be robust and integrated with greenhouse crop management practices [1]. The use of smart systems and technologies with mechanization, automation, and robotic applications can help improve the resource use efficiency and productivity in controlled environment agriculture (CEA) systems.

With the advancements in computers and sensors, micro-precision technology has been available for controlled environment plant production. The micro-precision technology does not always mean high engineering precision, rather it refers to an enabling technology to first identify what, how much, and when a resource is needed by the plants and then performs the action required to meet the identified quantitative and qualitative needs as precisely as possible. Some of these techniques and technologies are invasive and require contact measurements. It can be feasible to implement computational intelligence (CI) techniques to predict the most important and widely used plant morphological parameters such as plant growth mode or fruit growth modes for adjusting the operation of a greenhouse production system. Or, a more complete system can be developed to characterize the plant growth modes including quantitative and qualitative morphological features such as color, shape of leaves, flowers and plant head currently used by greenhouse growers. This can help capture the onset of undesired growth modes [2]. Therefore, the applications of CI techniques and automation with CEA plant production through real-time plant sensing and monitoring, desirably with non-invasive and non-contact capabilities, are needed [3].

Computer vision can be used to extract various information from a targeted object including morphological (size, shape, texture), spectral (color, temperature, moisture), and temporal data (growth rate, development, dynamic change of spectral and morphological states). Previous efforts of computer vision and sensing have been successful in determining plant status by monitoring a single leaf [4–7], or a single plant [8–12]. However, monitoring and sampling from the crop as a canopy are more desirable [13,14].

For commercial production settings, it is more advantageous to develop a real-time plant canopy health, growth and quality monitoring system with multi-sensor platforms. This can be achieved simply by a sensing system equipped with a multi-sensor platform moving over the canopy and ultimately using plants as "sensors" to communicate their true status and needs. Such systems can be used to detect crop deviations from normal development and crop stress (i.e., nutrient deficiencies or diseases). However, improved reliability, accuracy, rugged, and less expensive sensing systems in various aspects of crop production are in demand for better and more efficient site-specific management in crop production. Furthermore, increased sources of data provide more information and achieve a better performance. That is why, a multi-sensor-based data fusion strategy to allow a better interpretation of the region of interest or target than using an individual sensor alone is more desirable [15].

Knowing the value-added benefits of the real-time plant monitoring systems, researchers have paved the way for the commercialization of robotic machine vision systems to be implemented within greenhouse and growth chamber settings. The HortiMaX (http://www.hortimax.com) CropView system allows the grower to capture images of a single location in their plant canopy 24 hours a day, 7 days a week and time-stamped the images to corresponding greenhouse climatic data/events. The grower can only view a handful of plants within the image, not the entire plant canopy. Also this system does not extract plant or canopy features to quantitatively determine overall plant growth and status over time. In other words, if there is a plant-related problem, the trend of this issue is not identified until the grower visually identifies the problem themselves, typically when it is too late. Interest has been growing in high-throughput phenotyping systems. More accurate phenotyping systems and strategies are necessary to enable high-resolution mapping and genome-wide association studies and genomic selection models in crop improvement effort. Thus, the goal of modern phenotyping must be to increase precision, accuracy, and throughput of phenotypic estimations at all levels of biological organization. However, the costs and labor associated with the process must be minimized by automation, remote sensing, enhanced data integration and analysis [16]. LemnaTec (http://www.lemnatec.com), on the other hand, provides several Scanalyzer products, which monitors the plant as a continuum by automatically positioning the plant or camera to designated locations for controlled imagery and analysis. The level of accuracy from the Scanalyzer promotes the high precision required for plant phenotyping on a broad level. Due to the costs and small-scale design, this system is mainly for laboratory and growth chamber phenotyping settings, which is not practical for plant production on a commercial scale. To combat this disadvantage, LemnaTec offers a larger model, Scanalyzer Field, which offers similar precision for field scale operations. The Scanalyzer Field acquires plant imagery in three dimensions as well as associating the imagery with measured environmental conditions. This product does offer the complexity needed for the monitoring of plant production commercial operations however the information has not been available for the system performance on how the camera system deals with environmental variability.

There has been increasing interest from research and commercial greenhouse operation settings for non-invasive and non-contact real time crop monitoring and diagnostic systems. The changes in plant color, morphology, thermal features can be indicative of plant disease or stresses; therefore, monitoring the crop and analyzing these features in real time and providing qualitative and quantitative information to the growers can help them prevent damage to the crops, manage resources optimally, better monitor all aspects of the plant growth, and improve overall production quality. Therefore, this study was aimed at designing and implementing a computer vision-guided plant monitoring system, which can be used in real-time crop diagnostics dealing with the uncertainty of environmental light characteristics using

color, texture, crop indices, crop temperature, and temporal changes of the extracted features. This paper describes the system components, design, and an example implementation of the developed system. The remainder of this paper is organized as follows: Sect. 1.1 describes the details of the hardware of the robotic camera system, image processing and feature extraction process. Results of the camera positioning, image processing and feature extraction, and an example application of the developed system are discussed in Sect. 2. Section 3 provides conclusions and outline of the future work.

1.1 Overall system hardware, layout and signal processing

Growers have expressed an interest to see as much detail about their growing domain as possible and automated high-throughput phenotyping has been gaining interest as well for research applications. Thus, such applications demand for capturing and generating high resolution images, allowing the grower and operator to see their plants in high resolution with detailed information from extracted crop features. With a digital camera, sequential images, with an overlapping region of interest, can be stitched together to generate high-resolution, panoramic images. A robotic positioning system can be used to place these digital cameras to designated locations, such that the acquired images can be automatically stitched. Once a panoramic image has been generated, the plant regions can be separated from the background for extracting significant features and their analysis. In this study, the designed and constructed plant monitoring system consisted of five main components: (1) a stepper motor-driven camera positioning system, (2) an image acquisition system, (3) a data logger, monitoring root and aerial zone of the growing environment, (4) a dynamic Structured Query Language (SQL) database module for data storage, and (5) a host computer (PC) running the collection, processing, storage, and analysis functions. Figure 1 illustrates the connectivity of the system components and Fig. 2 identifies the flow diagram of the system developed for plant sensing and monitoring.

This study was developed in a research greenhouse at The University of Arizona, Controlled Environment Agriculture Center (Tucson, Arizona). A host computer (PC) was used for operational control of the plant monitoring system, stored in a custom built insulated cabinet whose internal environment (controlled by an air-conditioning unit) was specifically controlled for computer equipment (Fig. 3). The climate controlled cabinet also housed the stepper motor drivers, a data logger (to monitor the plant's root-zone and aerial environments), network-based external hard drive, and a network switch (to allow remote access to the computer and stored data). The program for the plant health monitoring system was custom built, written with Microsoft's Visual Studio 2010 in the VB.NET language. Some of the image processing tools were used from the AForge.NET library (http://www.aforgenet.com) and Emgu CV, a .NET wrapper for the OpenCV image processing library (http://www.emgu.com).

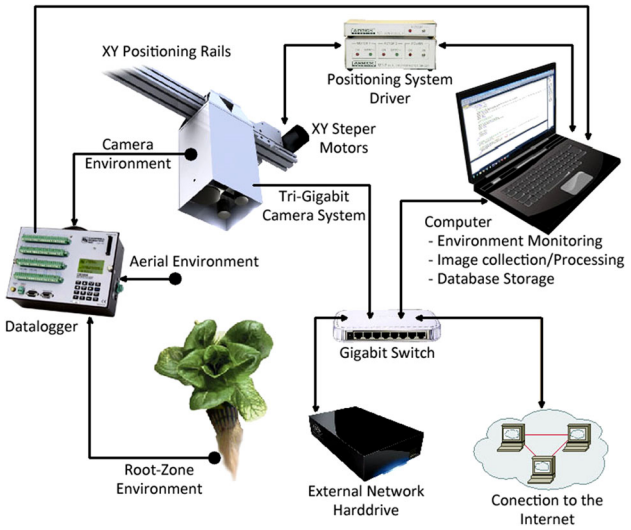

Fig. 1 Computer vision-guided crop diagnostics system components overview

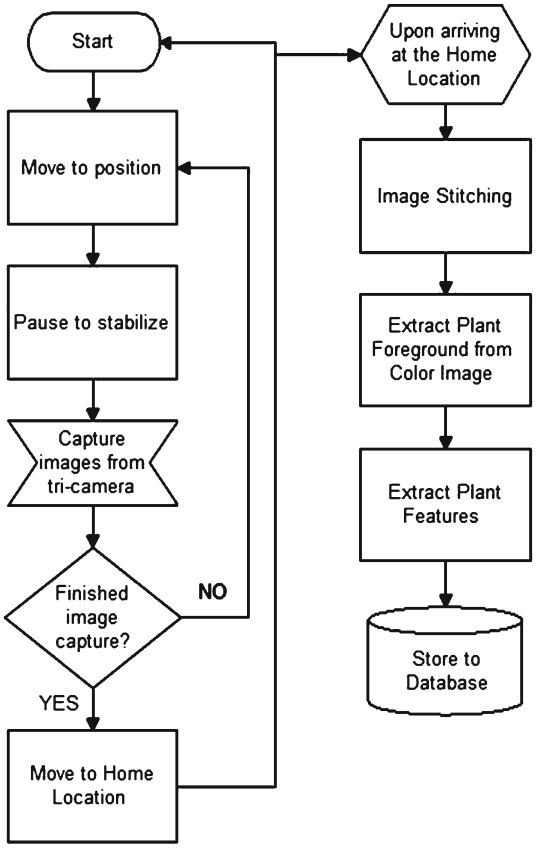

Fig. 2 Overall signal processing flow diagram

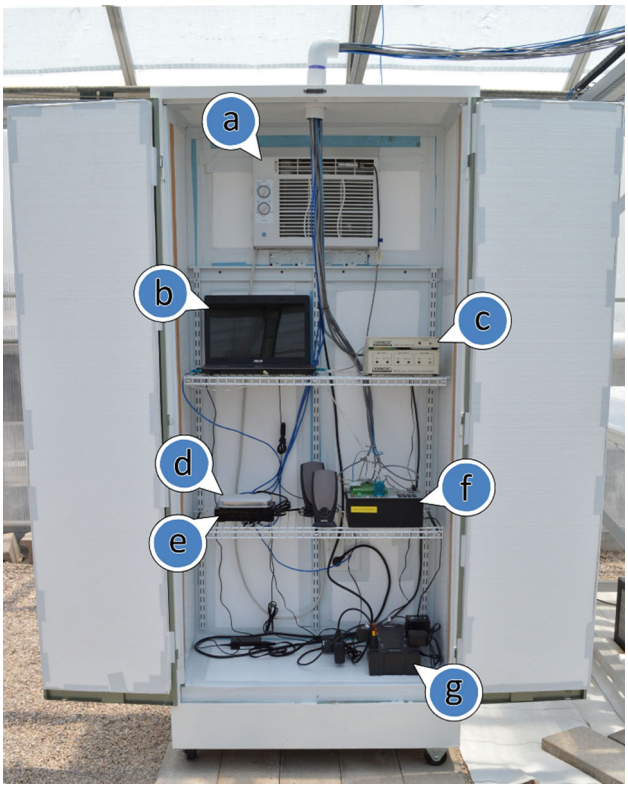

Fig. 3 Computer equipment cabinet located within the greenhouse. *a* Air conditioning unit, *b* host computer, *c* USB stepper motor drivers, *d* GigE switch, *e* external network hard drive, *f* Campbell Scientific CR3000 data logger, *g* battery backup power supply

1.2 Robotic camera positioning system

The robotic camera positioning system consisted of three joined rails. Two parallel beams defined the *y*-axis coordinate (Fig. 4b) and the third beam crossing perpendicular on top of the two *y*-axis beams formed the *x*-axis coordinate (Fig. 4c). Together, these three beams in association with two more side beams built a 152.4 × 152.4 cm square frame allowing the camera platform to be positioned anywhere within this *xy*-coordinate system, above the crop canopy in the NFT system.

Two stepper motors (MD2-b, Arrick Robotics Inc., Tyler, TX, USA) powered the robotic camera positioning platform in the *xy*-coordinate system (Fig. 4d). Both motors were operated by a stepper motor driver (MD-2, Arrick Robotics, Tyler, TX, USA) connected to a driver controller (C4, Arrick Robotics, Tyler, TX, USA), which acted as the communications device between the host computer and the stepper motor driver. This computer sent movement commands to the C4 hub activating and monitoring the movement of the stepper motors. Once the movement command ended, the C4 hub replied to the computer with a "movement finished" statement, identifying that the computer could execute the next task.

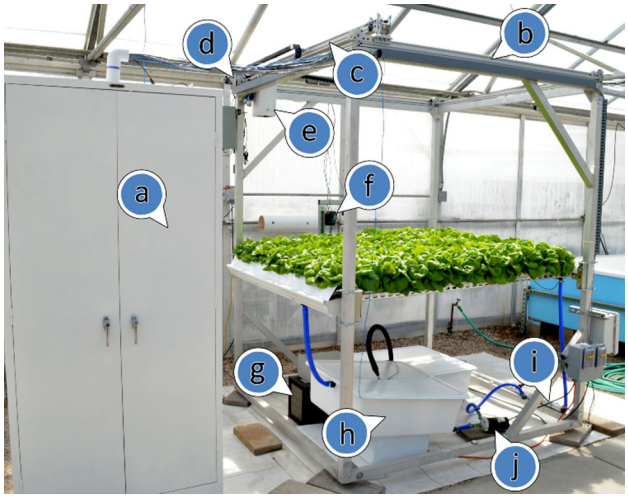

Fig. 4 Complete NFT growing system setup within the greenhouse. *a* Computer equipment cabinet, *b* *y*-axis positioning rail, *c* *x*-axis positioning rail, *d* two stepper motors one for each the *x* and *y*-axis rails, *e* tri-camera housing, *f* aerial environment sensors, *g* nutrient solution chiller, *h* nutrient solution reservoir, *i* root-zone environment sensors, *j* external irrigation pump

1.3 Image acquisition

The imaging unit consisted of three GigE vision cameras (tri-cameras): (1) color camera with a built-in NIR blocker (DFK 23G445, Imaging Source, Charlotte, NC, USA), (2) grayscale camera (DMK 23G445, Imaging Source, Charlotte, NC, USA) with NIR 850 nm bandpass-filter (67-853, Edmund Optics, Barrington, NJ, USA), and (3) thermal camera (A325, FLIR, Wilsonville, OR, USA). Each camera is powered with an external power supply adapter and communicated with the host computer through the network switch. The color and NIR cameras were equipped with a machine vision lens whose focal length is 8.50 mm and a field of view of 32.7° (NT58-000, Edmund Optics, Barrington, NJ, USA). The color and NIR cameras both generated an image of size 1280 × 960 pixels and each picture is saved as a jpeg with 95 % quality, which was found to have an acceptable compression with nearly no loss of detail. The thermal camera, with focal length of 18 mm and a field of view of 25°, generated a 2D image array with 320 × 240 pixels infrared resolution. Because the thermal camera detects the object's thermal radiance (in the thermal range 7.5–13 μm), the thermal resolution of detection is 0.01 K for each cell value within the 2D array. Each type-Single cell value is multiplied by 100 to convert the temperature value into an integer value which is then converted to a 3-Byte value array. The 3-byte arrays are split into individual bytes for each to be stored into an image's R-G-B channel. The resulting image was saved as a lossless bitmap image, with the Portable Network Graphics format, which is not an actual image but instead, a place-holder for the larger image stitching to occur. After image stitching, the

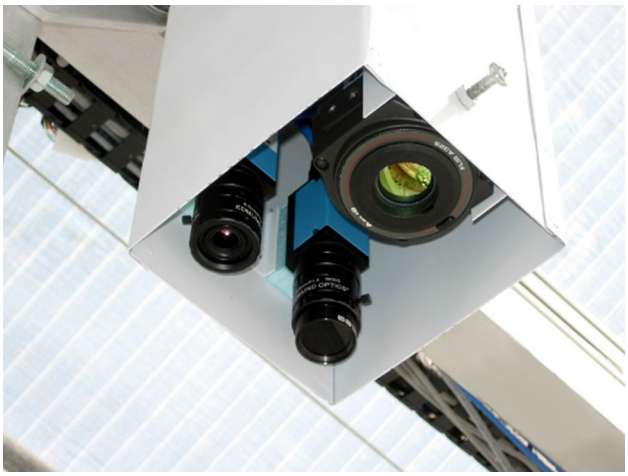

Fig. 5 Tri-camera housing with *color*, NIR, and thermal cameras (color figure online)

3 bytes (from the R-G-B channels) are then converted back to a temperature value.

The tri-camera housing (Fig. 5) was custom built from sheet metal. A cooling fan was attached at the base (top side), where the camera housing is connected to the positioning system. This cooling fan serves as two purposes: (1) to move air past the cameras to ensure they do not overheat and (2) to move dust down away from the camera lenses. The positioning of each camera was designed so that each camera lens is aligned at the same horizontal plane and height.

1.4 Panoramic image stitching

Due to the distortions the lens projects onto the imaging sensor, overlapping regions from images were not aligned (Fig. 6a). The distortions were calculated and removed from the image through image rectification, which improved the overall image alignment (Fig. 6b). Image distortions were identified by taking several pictures of a checkerboard. The checkerboard had straight and parallel lines which, when mapped, were used to identify the image distortions. The camera calibration process was performed at the beginning of the experiment using the procedures detailed by Sturm and Maybank [17].

After correcting for the lens distortions on each collected image, the images were then aligned to each other based on the sequential order the images were acquired. During image acquisition, the *xy* positioning system consistently moved to the same locations, allowing the overlapped regions to be constant (dark regions in Fig. 6a, b). The camera system's movement was correlated to image displacements and was recorded as a change in the image's *x* and *y* location. This correlation was calculated by knowing the horizontal movement of the cameras and translating the movement to pixel-wise displacements. All images with their respective displaced *x*–*y* location were applied to a stitching function, which automatically blended the images together forming a single large panoramic image (Fig. 6c).

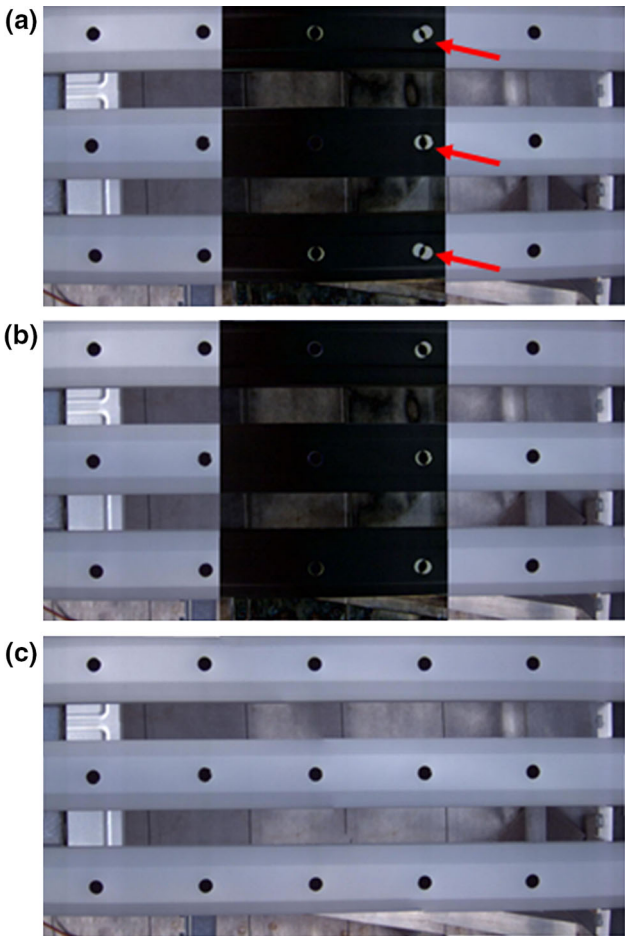

Fig. 6 Stitching alignments showing *dark* regions in the middle identify good overlapping regions. **a** Unrectified images, **b** rectified images, **c** stitched rectified images. *Red arrows* indicate misalignment due to image distortions (color figure online)

Various optimization techniques can be used for a seamless panoramic appearance. Stitching optimization techniques evaluate the overlapping regions within the images, identifying highly correlated regions as the best location for blending one image into the next. Due to the inconsistencies of the lighting conditions as well as the image variances between the three digital cameras, no stitching optimization was used in the present study. The blending technique used was a transparency gradient of an image's overlapping region. This ensured that the images were constantly aligned, from one panoramic alignment to the next. The reason for using a transparency gradient approach was because as the plants moved due to biotic movement or grew from one image to the next image (in 10 min interval), any stitching algorithm was not consistent with aligning the plant's shape. Therefore, the transparent blending technique was found to be improving the plant alignment with the series of panoramic image.

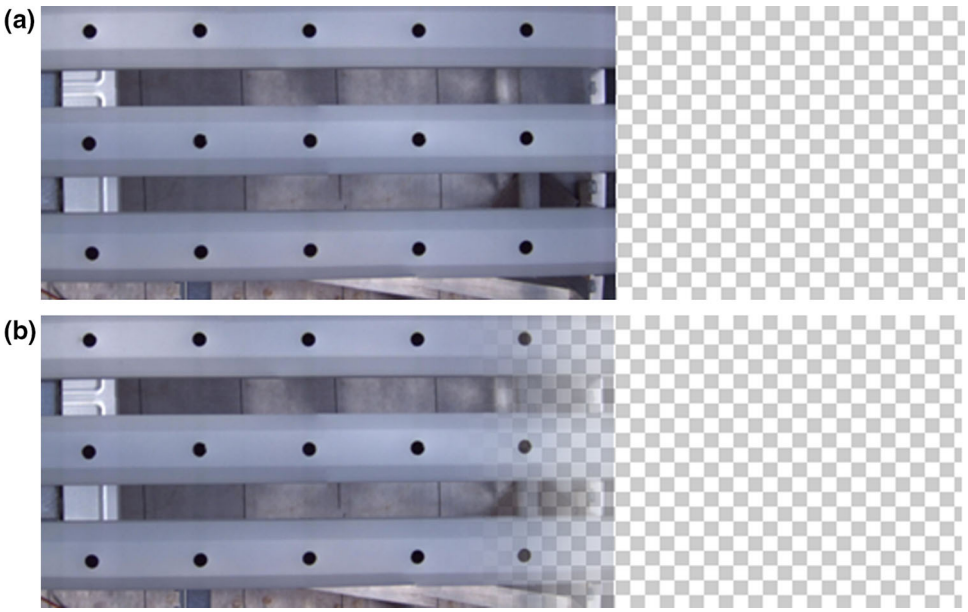

Fig. 7 Transparent gradient approach used for image stitching

Figure 7 illustrates the transparent gradient approach. Two images were aligned on top of each other, the NFT channels on the left and the checkerboard image to the right (Fig. 7a). The transparent gradient was calculated and applied to the alpha channel of any image but only within the overlapping region. Figure 7b shows the result of the blending technique or the transparent gradient, blending one image into the next.

All image stitching was automatically done through command-prompt scripts from PanoTools (http://wiki.panotools.org) but the image rectification and alignment parameters (including image registration) were initially created through the desktop software, Hugin Version 2012.0.0 (http://hugin.sourceforge.net). Hugin allows a user to collect information regarding a panoramic project and stores the data into a project file for use by command-line tools. The tools are a part of the pano-tools package (http://panotools.sourceforge.net) allowing a user to generate panoramic images. There was no stitching algorithm performed. It was only a transparent gradient of the over lapping regions. The transparency was performed by modifying the alpha channel of an ARGB image. With Hugin, camera parameter and image alignment project files were manually created once and applied to each image collection run, allowing the creation of panoramic images dynamically.

The stitching procedure began with acquiring images to be stored to the hard drive, within appropriate named folders. This ensured the ability to revisit the stored images if any questions arise regarding the final stitched image. After the positioning system completed the movement pattern and all cameras acquired the images, the controlling software then began to stitch the image collections together. Through the custom created software's automation, the folders were copied with the Hugin project files and the software called the command-prompt scripts to rectify the images and initiated the stitching. Figure 8 illustrates an example of the tri-camera stitched canopy images, layered so that the plant regions are aligned for feature extraction and analysis. The top-most layer is the resulting extracted plant blobs (discussed in Sect. 1.5). The resulting images were 4340 × 3708 pixels and at 72 dpi, thus this resulting image represented a region of interest (ROI) of 1.53 × 1.31 m in size from the crop production domain.

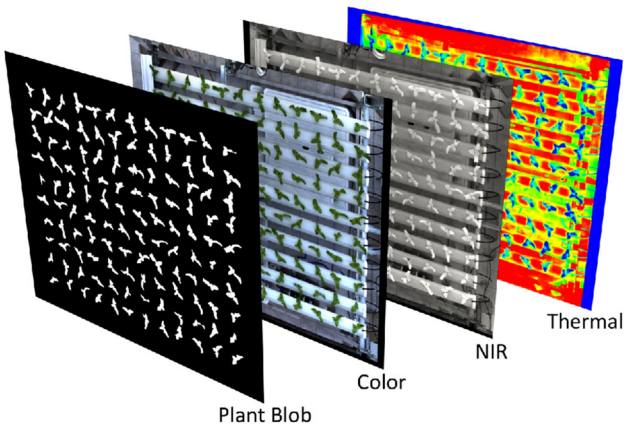

Fig. 8 Stitched canopy images from the tri-camera system, the *first top-most layer* is the extracted plant blob layer

1.5 Image analysis and feature extraction

Image segmentation, partitioning of an original image into various segments, is important for various image processing applications such as object identification and pattern recognition. Once the crop canopy's panoramic color image has been stitched, it was necessary to identify the plant only-regions within this panoramic image. Therefore, the only plant (or

plant canopy) portion of the image was segmented from the overall panoramic image. The extraction method used was a Hue–Saturation–Luminance (H–S–L) filtering which actively selects the plant's green color as foreground from the rest of the image as background, which was never green in color. The appropriate HSL filtering values were obtained based on preliminary processing and experimentation with collected images under varying lighting conditions. Based on preliminary analysis for best HSL ranges [Hue (50:120), Saturation (0.1:1.0), and Luminance (0.0:0.6)], the following formula was then used to obtain a binary image, extracting the plant foreground as white blobs.

$$\text{Blob} : P\,[i,\,j] = \text{if Color} : P[i,\,j] \in \begin{matrix}\text{Hue } (50:120)\\ \text{Sat } (0.1:1.0)\\ \text{Lum } (0.0:0.6)\end{matrix} \begin{matrix}\text{then } 1\\ \text{else } 0\end{matrix} \tag{1}$$

the designated monochromatic blob pixel (1 represents foreground, 0 represents background); Color: $P[i,\,j]$ is the designated color pixel located at $[i,\,j]$; Hue, Sat (Saturation), and Lum (Luminance) are each ranges that if the color pixel falls in these ranges it is considered as foreground.

With the image segmented into two regions, the image was again processed to remove small noises. To do this, a blob minimum-size analysis was performed, filtering out any unconnected blob that had a width and height size of 40×40 pixels or smaller. From this resulting monochromatic blob image, the plant morphology feature, top projected canopy area (TPCA), is extracted using the following formula:

$$\text{TPCA} : \sum_i \sum_j \text{Blob} : P\,[i,\,j] \tag{2}$$

where Blob: $P[i,\,j]$ is the designated monochromatic blob pixel (1 represents foreground, 0 represents background).

This focused plant blob image (top most layer in Fig. 8) was overlaid on top of each of the three images, using the white blob region to extract the plant-only portion from the corresponding images. For the color layer, the plant region was used to calculate the color features of the plant canopy. All colored pixels were averaged together to identify the overall plant (or canopy) color. The averaged color value was stored into the database for analysis as Red–Green–Blue (RGB), Hue–Saturation–Luminance (HSL), and Color Brightness which is a numerical representation of the color's brightness to the human eye [18].

A gray-level co-occurrence matrix was created by converting the color plant image to grayscale, capturing the spatial dependence of gray-level values contributing to the perception of the plant's texture [19]. Since the image texture is orientation dependent, four different matrices were calculated based on the different angles of pixel relativity (0°, 45°, 90°, and 135°). Each matrix was run through probability density functions to determine textural parameters. After analyzing the color features of the focused plant image, the textural features were then extracted. These extracted canopy textural features were [14,20]

$$\text{Entropy} : \sum_i \sum_j P\,[i,\,j] \log P\,[i,\,j] \tag{3}$$

$$\text{Energy} : \sum_i \sum_j P^2\,[i,\,j] \tag{4}$$

$$\text{Contrast} : \sum_i \sum_j (i-j)^2 P\,[i,\,j] \tag{5}$$

$$\text{Homogeneity} : \sum_i \sum_j \frac{P\,[i,\,j]}{1+|i-j|}, \tag{6}$$

where $P[i,\,j]$ is the probability density function with gray levels located at i and j.

The plant's NIR reflectivity was also extracted when the plant blob image was overlaid onto the NIR canopy image, averaged for the entire plant area and stored for analysis. A plant is highly reflective in the NIR band due to the internal cellular structure of a plant's leaf [21]. If a plant exhibits a stress, this internal leaf structure changes, resulting in a change of the NIR reflectivity. Analysis of this NIR value to the plant's Red channel value has been shown to be a good indicator of plant health [22–24]. Two relationships for NIR to other color comparisons were implemented: a reflectance ratio (SR—simple ratio) and the normalized difference vegetation index (NDVI). Relationships of the NIR value to other color values have also been evaluated (NIR-Green and NIR-Blue) as well as a unique relationship similar to the NDVI, the enhanced normalized difference vegetation index (ENDVI).

$$\text{SR} : \frac{\text{NIR}}{\text{Color}} \tag{7}$$

$$\text{NDVI} : \frac{\text{NIR} - \text{Color}}{\text{NIR} + \text{Color}} \tag{8}$$

$$\text{ENDVI} : \frac{(\text{NIR} + \text{Green}) - (2 \times \text{Blue})}{(\text{NIR} + \text{Green}) + (2 \times \text{Blue})}, \tag{9}$$

where NIR is the reflected NIR plant canopy value and Color is the reflected color plant canopy (Red, Green, or Blue channels).

Lastly, the plant blob image was overlaid onto the thermal canopy image, extracting the plant's average temperature to be stored and used for analysis. Analyzing a plant's temperature or mainly the plant's temperature regulating mechanism (the stomata cells) through transpiration, one can identify the plant's health and specifically responses to water stress [25]. When the stomata cells are open, carbon dioxide enters the plant while oxygen and water vapor leave the plant. The exiting of the water vapor provides two internal functions: (1) the process cools the plant and (2) the process causes suction, drawing up more water and nutrients from the root

system. When the plant is under stress, the function of the stomata cells reflects this stress and in turn alters the plant's overall temperature. By comparing the plant temperature to a known well-watered (un-stressed) plant temperature and a non-watered (stressed) plant temperature, a water-stress index (CWSI) or the overall stomatal conductance can be inferred to indicate the level of water stress in plant canopy [26–28]. The CWSI calculation was not performed in the current study; however, the key variables to calculate CWSI have been made available to the operator and for crop diagnostic and phenotyping applications. The developed crop monitoring system enabled monitoring and collection of a total of seventeen variables, as potential features to be analyzed and used for crop monitoring and diagnostics.

2 Camera positioning, image processing and feature extraction

2.1 Positioning system's movement

Based on the crop production system layout used in this study, it was found that the best movement pattern to execute was a zigzag pattern, making seven stops both in the x and y direction. This movement pattern resulted with a total of 49 acquired images from one camera. This pattern allowed a decent overlap of acquired images for image stitching and had an acceptable total travel time of 6 min and 28 s, moving over the entire growing domain. A specific movement speed was selected to ensure the motion stability of the camera platform. By increasing this speed, the total traveling time could have been improved but, in the long run, might affect this motion stability. Also, any increase of stops can lengthen the travel time but not improve the quality of the image stitching. Likewise, any decrease in stops can improve the movement time but decrease the stitching ability.

2.2 Image processing and feature extraction

After the camera system acquired the targeted 49 images, the host computer then stitched the images together to generate a large panoramic image. It took the system approximately 3.5 min to completely stitch all three of the tri-camera images. Once completed, the system then focused on generating the plant blob image from the completed color layer image. Through blob extraction and noise removal, the system took approximately 28 s to generate the plant blob image. With all four image layers created, the system then extracted the plant features from each layer to be stored within the database for analysis. This data extraction step took the system approximately 47 s to complete. From the start of image acquisition to the end of the data extraction, the entire process took the host computer approximately 11.2 min to complete.

With plant image analysis, it is necessary to segment the plant image into two regions: the focused plant as the foreground and everything else as the background. To easily identify the plant foreground, a uniform background of known color is implemented. Actively selecting this color as the background easily enables the ability to label the plant regions as the foreground [4,8,12]. When the background is unknown, researchers have developed strategies to focus on the plant region by subtracting the background from the image. For instance, a bi-class problem with Otsu's method was used with gray scale images [29]. A fixed zero threshold, unsupervised vegetation index with excess green minus excess red (ExG-ExR) was successfully demonstrated to separate plants and backgrounds for image sets obtained under greenhouse field lighting conditions [30]. An environmentally adaptive segmentation algorithm under hue–saturation–intensity color space was also proposed to consider the illumination variability effect [31]. Furthermore, a combined approach of statistical strategies based on information of the image through the intensity uniformity was used [32], ensuring that the background and foreground regions were appropriately labeled. One of the commonly used methods for performing plant foreground/background image thresholding has been Otsu's thresholding method [33]. This method assumes that the image is composed of two classes: a foreground and a background. Through statistical analysis of the image's weighted histogram, the threshold is identified to be the point where the smallest variances within these two classes exist. This approach has advantages as being an easy and fast speed method. However, as the plants grow, forming a full canopy, the method starts looking at identifying two classes within the full canopy, resulting in noisy images (Fig. 9, middle column). The segmentation method implemented in this study actively selects the green-plant color which proved to be more accurate at selecting the plant region despite their growth size (Fig. 9, right column). A drawback though is to ensure the background does not contain the targeted foreground color and that the focused plant regions are of a similar color.

One of the major challenges faced was shadows and inconsistent light conditions affecting information contained in the images (i.e., with the color plant image or plant NIR reflectivity). These environmental variations have even caused discrepancies with the plant blob extraction (Fig. 10a). In this study, we used a summation of previous plant blob images to automatically and continually identify plant regions. Whether a plant was detected or not, this summation ensured the plant region maintained the same location, allowing the environmental inconsistencies to be ignored from the plant extraction (Fig. 10b). This approach does not take into consideration that a plant may shrink slightly during its diurnal movements. Since this plant blob variance was significantly smaller than the overall plant size (Fig. 10b), it was, therefore,

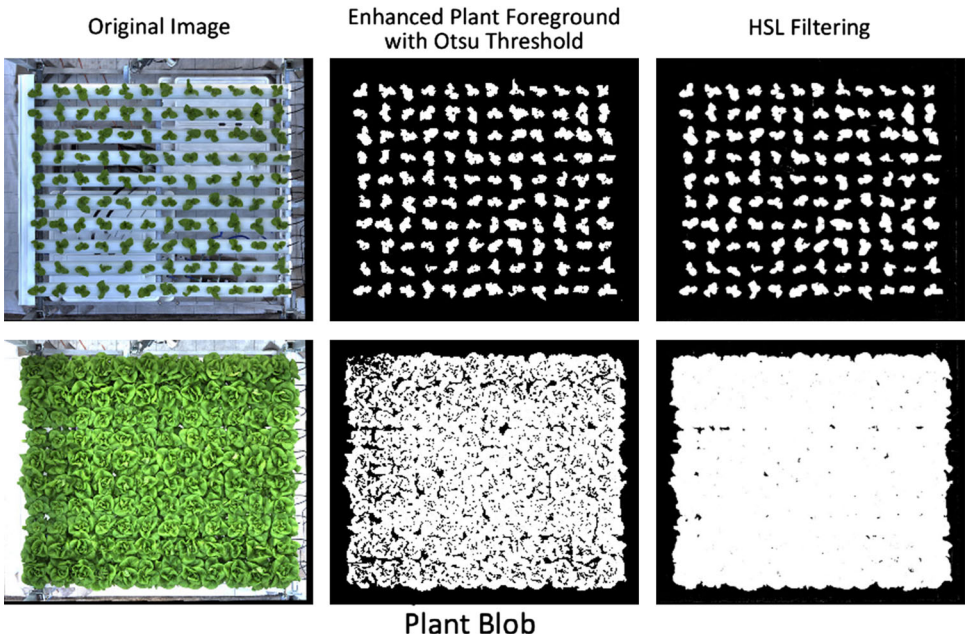

Fig. 9 Plant blob extraction examples. The *left column* is the original images, the *top* being seedlings, *bottom* being the full plant canopy. The *center column* is the plant extraction from the background based on the enhanced plant region with Otsu threshold method. The *right column* is the plant extraction from the background based on the HSL filtering

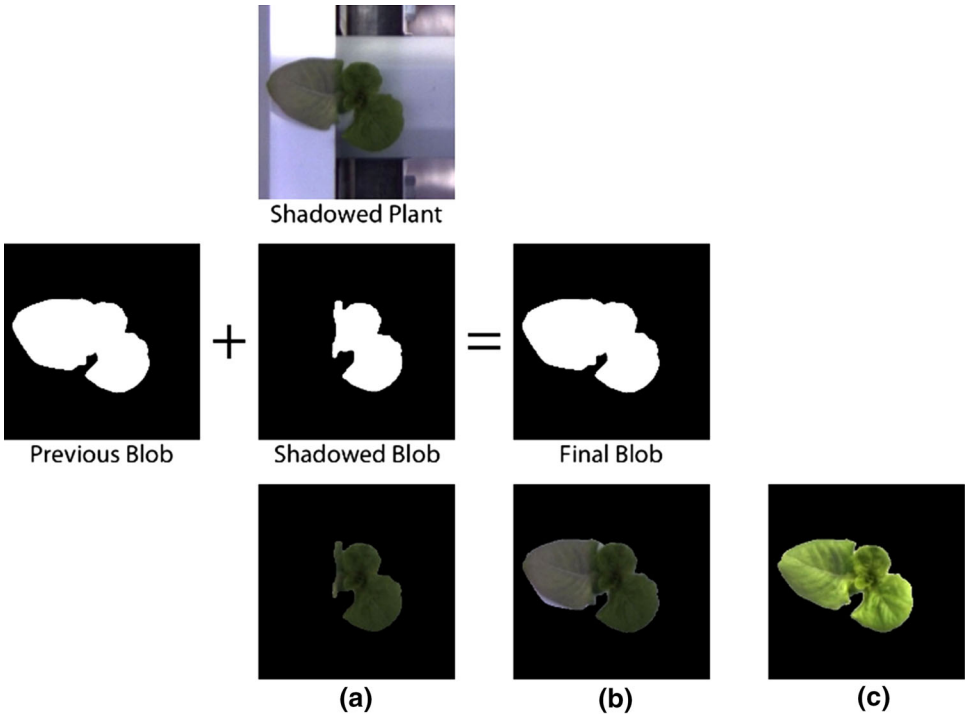

Fig. 10 Plant blob extraction method for handling unfavorable environmental conditions. **a** The original blob extraction overlaid onto the *color* image, **b** the improved plant blob overlaid onto the same *color* image giving an improved plant canopy extraction. Also to note, the plant blob is slightly larger than the actual plant. **c** A focused plant where the lighting conditions emphasize the plant's texture altering the perception of the plant at that specific moment of time (color figure online)

ignored in this study. However, if an unexpected adjustment to the NFT system occurs, while the imaging is running, then the overlaid plant canopy blob can have a large deviation and re-creation of this plant blob layer is needed in order to properly extract the plant features.

In addition to the environmental inconsistencies affecting the plant blob extraction, these inconsistencies were also reflected in the extracted features (Fig. 10b, c). Feature normalization or adjustment (i.e., shadow removal) based on the environmental conditions can be used to improve the feature's quality. In this study, frequent data collection and a moving-hourly average was used to cancel the environmental effects on the extracted features.

2.3 Crop monitoring application in greenhouse

An example of crop monitoring application with the developed system is provided in this section by illustrating its capability to monitor an NFT growing domain of 10 rows, each row with 12 lettuce plants, spaced approximately 15.2 cm apart (Fig. 4). The system started daily at 7 a.m. and ended at 6 p.m., acquiring canopy images every 10 min. Computer

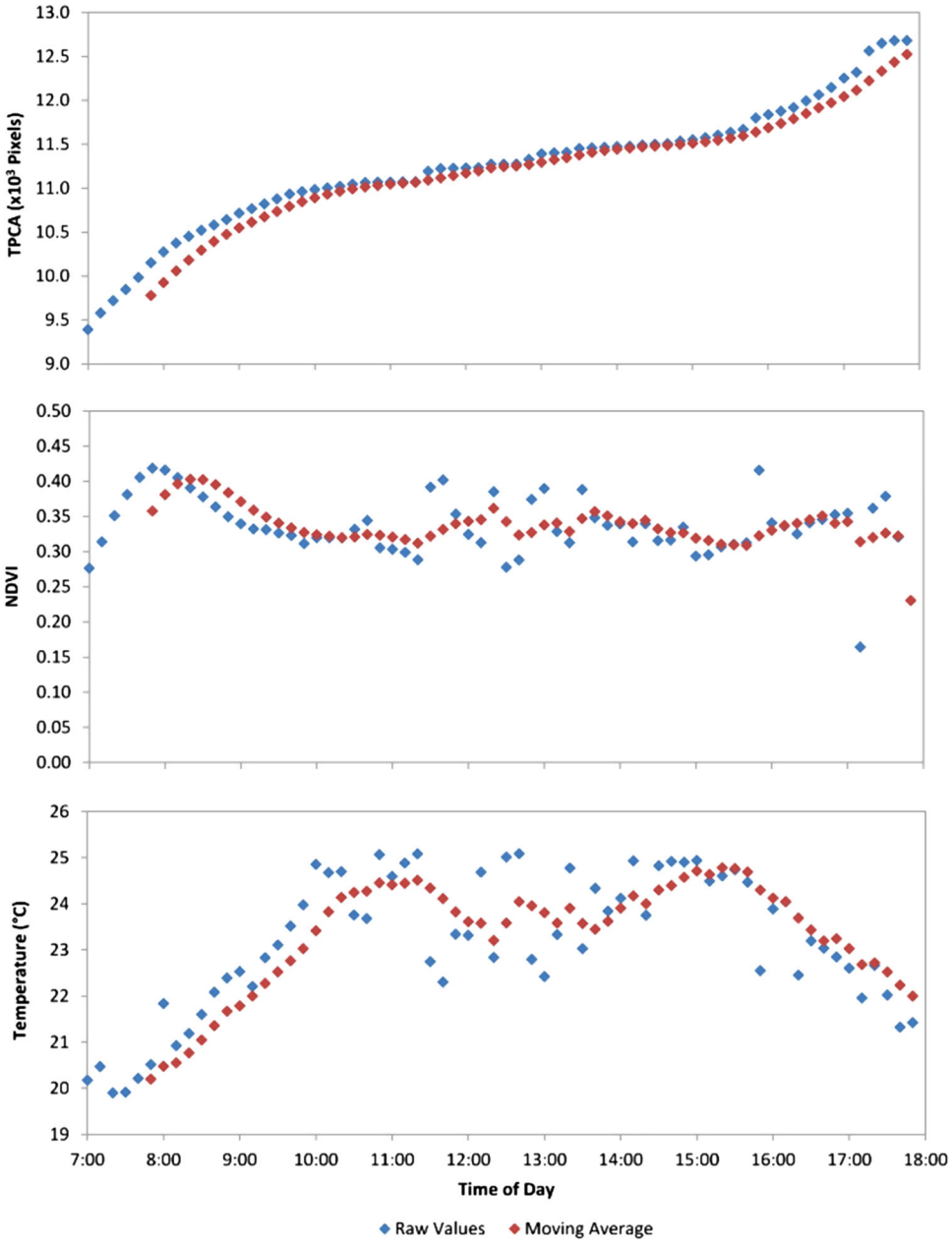

Fig. 11 Examples of the extracted plant features. The blue points represent the average of 120 plants at that specific time whereas the red points are a moving average of 6 points

vision system acquired total of seventeen crop related features; however, only three features (TPCA, NDVI and canopy temperature) of greenhouse grown lettuce crop over a one day period are presented in this study (Fig. 11) as example of system's capability for crop monitoring. Each data point is shown as an average of the 120 plants. The TPCA graph indicates an expected growth pattern from the healthy canopy as well as approximately a uniform NDVI value during the course of the day. The canopy temperature increases after sunrise as all the leaves are exposed to solar radiation, and it decreases due to evaporative cooling effect by transpiration during the noon and early afternoon hours in a fluctuating trend. Finally, the temperature decreases towards the end of the sunlight hours.

If a treatment (i.e., water stress) was to be applied, the crop monitoring system designed in this study can monitor the health and growth features temporally, identifying statistically significant changes between the control and treatment groups. For this, a methodology is required to accurately and timely determine the onset of stress or growth deviated from normal. Therefore, a multi-variable-based crop diagnostic methodology was developed to identify significant features separating the control (healthy) and treatment (water stressed) plant group, and indicated the locality of the stress for the operator. A result of this approach is shown in Fig. 12. The water stress was applied to four channels in the NFT production system; images were collected every 10 min interval and seventeen plant features were extracted. In addition to

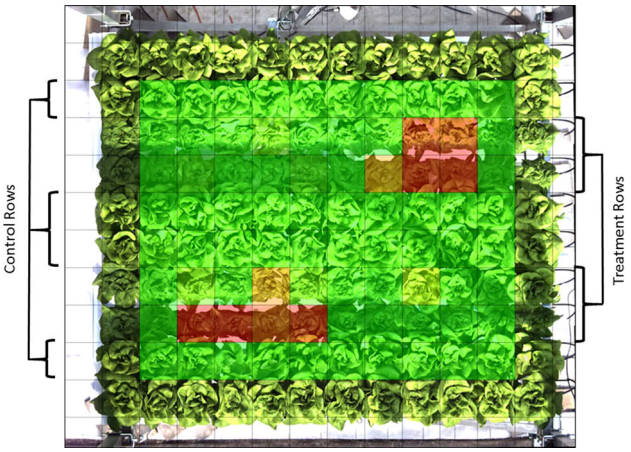

Fig. 12 Crop stress severity and locality identification based on multi-variable-based approach using crop features obtained from the computer vision system

seventeen plant features, temporal trend relationships were also calculated. The relationships obtained from plant features were used to identify ratios or changes from the daily first and the previous values, all based on a cell's moving one hour average value. The six plant feature-based relationships were: (1) the cell's average feature value, (2) a ratio of the current cell feature value to the cell's first feature value of the day, (3) a ratio of the current cell feature value to the cell's previous feature value, (4) the cell's variation from the first value of the day, (5) the cell's variation between the current feature value to the previous feature value, and (6) the cell's feature value's coefficient of variation, indicating the variation relative to cell's mean value. In addition to considering all collected raw values for the seventeen plant features, the analysis also evaluated the plant cell's value (cell was defined as each square region in the checker board pattern in Fig. 12) to previously stored values, aiding in the classification of the water stress and locality in each cell and the production domain. To achieve this, the multi-variable-based crop stress detection approach used statistical-based analysis for determining the level of water stress and its locality and generating a final canopy output image which indicated the level of water stress observation and locality with color coding (i.e., red-severe, orange-moderate, and yellow-low level). The details of the multi-variable-based crop diagnostics methodology will be published in another manuscript.

3 Conclusion

A machine vision-guided plant sensing and monitoring system was constructed to continuously monitor color, morphological, textural, and spectral (crop indices and temperature) features from a crop canopy. The developed system used a distributed processing hierarchy with motion control, image acquisition, and environmental data collection. Sources of reduced image quality and plant extraction accuracy were analyzed and quantified. The developed system can autonomously monitor and extract Red–Green–Blue, Hue–Saturation–Luminance, color brightness as color features; entropy, energy, contrast, and homogeneity as textural features; TPCA as a morphological feature; NIR reflectivity, and thermal radiation from a single plant or a plant canopy. Thus, a total of seventeen features are temporally collected and provided for the operator by the system. The machine vision system extracted these identified plant features which can be used to determine the overall plant growth and health status, but is capable of analyzing a much larger range of parameters for other plant phenotyping applications (i.e., perimeter, centroid, diameter etc). The system is an adaptable sensing and monitoring platform which can collect greenhouse aerial, non-contact crop related, and crop root zone data enabling to establish the monitoring of a plant's environment as a seamless continuum. This can certainly help analyzing crop and microclimate interactions more closely and can lead to improved greenhouse and crop resource use management practices. Combining the systems capability with a decision support system can assist in dealing with identifying complexity of the crop stress symptoms and an increased control of the overall plant growth environment, which can potentially improve resource use efficiency in controlled environment crop production systems.

Acknowledgments The authors would like to thank Neal Barto, Myles Lewis, and Charley Defer for assisting with the construction of the machine vision system. This research was supported by NASA Ralph Steckler Space Colonization Research and Technology Development Program Project funds (NNX10AC28A) and by the Technology and Research Initiative Fund (TRIF) Imaging Fellowship program funding.

References

1. Helmer, T., Ehret, D.L., Bittman, S.: CropAssist, an automated system for direct measurement of greenhouse tomato growth and water use. Comput. Electron. Agric. **48**, 198–215 (2005)
2. Fitz-Rodriguez, E., Giacomelli, G.A.: Yield prediction and growth mode characterization of greenhouse tomatoes with Neural Networks and Fuzzy Logic. Trans. ASABE **52**(6), 2115–2128 (2009)
3. Kacira, M., Sase, S., Okushima, L., Ling, P.P.: Plant response based sensing and control strategies in sustainable greenhouse production. J. Agric. Meteorol. Japan **61**(1), 15–22 (2005)
4. Seginer, I., Elster, R.T., Goodrum, J.W., Rieger, M.W.: Plant wilt detection by computer-vision tracking of leaf tips. Trans. ASAE **35**(5), 1563–1567 (1992)
5. Meyer, G.E., Troyer, W.W., Fitzgerald, J.B., Paparozzi, E.T.: Leaf nitrogen analysis of poinsettia (Euphorbia Pulcherrima Will D.) using spectral properties in natural and controlled lighting. Appl. Eng. Agric. **8**(5), 715–722 (1992)
6. Shimizu, H., Heins, R.D.: Computer-vision-based system for plant growth analysis. Trans. ASAE **38**(3), 959–964 (1995)

7. Revollon, P., Chasseriaux, G., Riviere, L. M., Gardet, R.: The use of image processing for tracking the morphological modification of Forsythia following an interruption of watering. In: Proceedings of International Conference on Agricultural Engineering, Oslo, pp. 872–873 (1998)
8. Hetzroni, A., Miles, G.E., Engel, B.A., Hammer, P.A., Latin, R.X.: Machine vision monitoring of plant health. Adv. Space Res. **14**(11), 203–212 (1994)
9. Ling, P.P., Giacomelli, G.A., Russell, T.P.: Monitoring of plant development in controlled environment with machine vision. Adv. Space Res. **18**(4–5), 101–112 (1996)
10. Kurata, K., Yan, J.: Water stress estimation of tomato canopy based on machine vision. Acta Hortic. **440**, 389–394 (1996)
11. Murase, H., Nishiura, Y., Mitani, K.: Environmental control strategies based on plant responses using intelligent machine vision technique. Comput. Electron. Agric. **18**, 137–148 (1997)
12. Kacira, M., Ling, P.P., Short, T.H.: Machine vision extracted plant movement for early detection of plant water stress. Trans. ASAE **45**(4), 1147–1153 (2002)
13. Leinonen, I., Jones, H.G.: Combining thermal and visible imagery for estimating canopy temperature and identifying plant stress. J. Exp. Bot. **55**, 1423–1431 (2004)
14. Ushada, D., Murase, H., Fukuda, H.: Non-destructive sensing and its inverse model for canopy parameters using texture analysis and artificial neural network. Comput. Electron. Agric. **57**, 149–165 (2007)
15. Lee, W.S., Alchanatisb, W., Yang, C., Hirafuji, M., Moshoue, D., Li, C.: Sensing technologies for precision specialty crop production. Comput. Electron. Agric. **74**, 2–33 (2010)
16. Cobb, J., Genevieve, D.: Next-generation phenotyping: requirements and strategies for enhancing our understanding of genotype-phenotype relationships and its relevance to crop improvement. Theor. Appl. Genet. **126**, 867–887 (2013)
17. Sturm, P., Maybank, S.: On plane-based camera calibration: a general algorithm, singularities, applications. In: Proc. IEEE Conf. Computer Vision and Pattern Recognition, pp. 432–437 (1999)
18. Bezryadin, S., Bourov, P., Ilinih. D.: Brightness calculation in digital image processing. In: Proceedings of International Symposium on Technologies for Digital Fulfillmen, Las Vegas (2007)
19. Jain, R., Kasturi, R., Schunck, B.J.: Machine Vision. McGraw-Hill, New York (1995)
20. Zheng, C., Sun, D.W., Zheng, L.: Recent applications of image texture for evaluation of food qualities—a review. Trends Food Sci. Technol. **17**, 113–128 (2006)
21. Penuelas, J., Filella, I.: Visible and near-infrared reflectance techniques for diagnosing plant physiological status. Trends Plant Sci. **3**, 151–156 (1998)
22. Gamon, J.A., Field, C.B., Goulden, M.L., Griffin, K.L., Hartley, A.E., Joel, G., Peñuelas, J., Valentini, R.: Relationships between NDVI, canopy structure, and photosynthesis in three Californian vegetation types. Ecol. Appl. **5**(1), 28–41 (1995)
23. El-Shikha, D., Waller, P., Hunsaker, D., Clarke, T., Barnes, E.: Ground-based remote sensing for assessing water and nitrogen status of broccoli. Agric. Water Manag. **92**, 183–193 (2007)
24. Ryu, Y., Baldocchi, D., Verfaillie, J., Ma, S., Falk, M., Ruiz-Mercado, I., Hehn, T., Sonnentag, O.: Testing the performance of a novel spectral reflectance sensor, built with light emitting diodes (LEDs), to monitor ecosystem metabolism, structure and function. Agric. For. Meteorol. **150**, 1597–1606 (2010)
25. Hetherington, A.M.: Plant physiology: spreading a drought warning. Curr. Biol. **8**(25), 911–913 (1998)
26. Jones, H.G.: Use of infrared thermometry for estimation of stomatal conductance as a possible aid to irrigation scheduling. Agric. For. Meteorol. **95**, 139–149 (1999)
27. Jones, H.G., Stoll, M., Santos, T., Sousa, C., Chaves, M., Grant, O.: Use of infrared thermography for monitoring stomatal closure in the field: application of grapevine. J. Exp. Bot. **53**(378), 2249–2260 (2002)
28. Cohen, Y., Alchanatis, V., Meron, M., Saranga, Y., Tsipris, J.: Estimation of leaf water potential by thermal imagery and spatial analysis. J. Exp. Bot. **56**(417), 1843–1852 (2005)
29. Ling, P.P., Ruzhitsky, V.N.: Machine vision techniques for measuring the canopy of tomato seedling. J. Agric. Eng. Res. **65**(2), 85–95 (1996)
30. Meyer, G.E., Neto, J.C.: Verification of color vegetation indices for automated crop imaging applications. Comput. Electron. Agric. **63**, 282–293 (2008)
31. Ruiz-Ruiz, G., Gomez-Gil, N., Navas-Gracia, L.M.: Testing different color spaces based on hue for the environmentally adaptive segmentation algorithm (EASA). Comput. Electron. Agric. **68**(1), 88–96 (2009)
32. Guijarro, M., Pajares, G., Riomoros, I., Herrera, P., Burgos-Artizzu, X., Ribeiro, A.: Automatic segmentation of relevant textures in agricultural images. Comput. Electron. Agric. **75**, 75–83 (2011)
33. Otsu, N.: A threshold selection method from gray-level histogram. IEEE Trans. Syst. Man Cybern. **9**(1), 62–66 (1979)

David Story received his Ph.D. degree from Department of Agricultural and Biosystems Engineering at the University of Arizona in 2013 where he worked in the Advanced Sensing & Climate Control Lab for Sustainable CEA Systems. Dr. Story received his bachelors' degree in Computer Sciences from Northern Illinois University in 2005 and his master's degree in Agricultural and Biosystems Engineering in 2009 from University of Arizona. His research interest included computer vision-guided systems for plant monitoring.

Murat Kacira received his Ph.D. in (2000) and Master's (1996) degrees in Food, Agricultural and Biological Engineering from The Ohio State University. Dr. Kacira received his bachelors' degree in Agricultural Engineering from Cukurova University. He is the director of the Advanced Sensing & Climate Control Lab for Sustainable CEA Systems at the University of Arizona. His research interest include computer vision-guided systems for plant monitoring, computational fluid dynamics based aerodynamics analysis of controlled environment agriculture (CEA) systems, and alternative energy use in CEA systems.